Supporting Information

A small molecule inhibitor that stabilizes the autoinhibited conformation of the oncogenic tyrosine phosphatase SHP2

Xiaoqin Wu[1, †], Gang Xu[2, †], Xiaobo Li[1, 2, †], Weiren Xu[2], Qianjin Li[1], Wei Liu[2], Karen A. Kirby[3], Mignon L. Loh[4], Jun Li[5], Stefan G. Sarafianos[3], and Cheng-Kui Qu[1, 2, *]

[1] Department of Pediatrics, Division of Hematology/Oncology, Aflac Cancer and Blood Disorders Center, Children's Healthcare of Atlanta, Emory University School of Medicine, Atlanta, GA 30322, USA. [2] Department of Medicine, Division of Hematology and Oncology, Case Comprehensive Cancer Center, Case Western Reserve University, Cleveland, OH 44106, USA. [3] Department of Pediatrics, Laboratory of Biochemical Pharmacology, Emory University School of Medicine, Atlanta, GA 30322, USA. [4] Department of Pediatrics, Division of Pediatric Hematology-Oncology, University of California, San Francisco, San Francisco, CA 94122, USA. [5] School of Pharmacy, Anhui Medical University, Hefei, 230032, China.

[†] These authors contributed equally to this work.

Table of Contents

Other supplementary information for review.

Top hits from the initial screening. Top 90 structures identified from the initial virtual screening of the NCI database (in a separate file).

PAINS results. PAINS results of the top 100 hits from the initial database screening and the derivatives of NSC681129 (in a separate file).

PDB file 1. Structure of the **1**/SHP1 complex in the PDB format (in a separate file).

PDB file 2. Structure of the **1**/SHP2 complex in the PDB format (in a separate file).

Molecular formula strings of 1. CSV file of molecular formula strings of **1** (in a separate file).

Proton NMR data of 1. 1 in dimethyl sulfoxide-d6 (4 mM) was analyzed using Bruker Ascend 400 MHz NMR apparatus (in a separate file).

NMR results of other synthesized derivative compounds. LY1-LY5 and LY7-LY10 in dimethyl sulfoxide-d6 (4 mM) were analyzed using Bruker Ascend 400 MHz NMR apparatus (in a separate file).

HPLC data of all synthesized derivative compounds. LY1-LY10 in methanol (50 μg/mL) were analyzed using Shimadzu HPLC-PDA/UV (in a separate file).

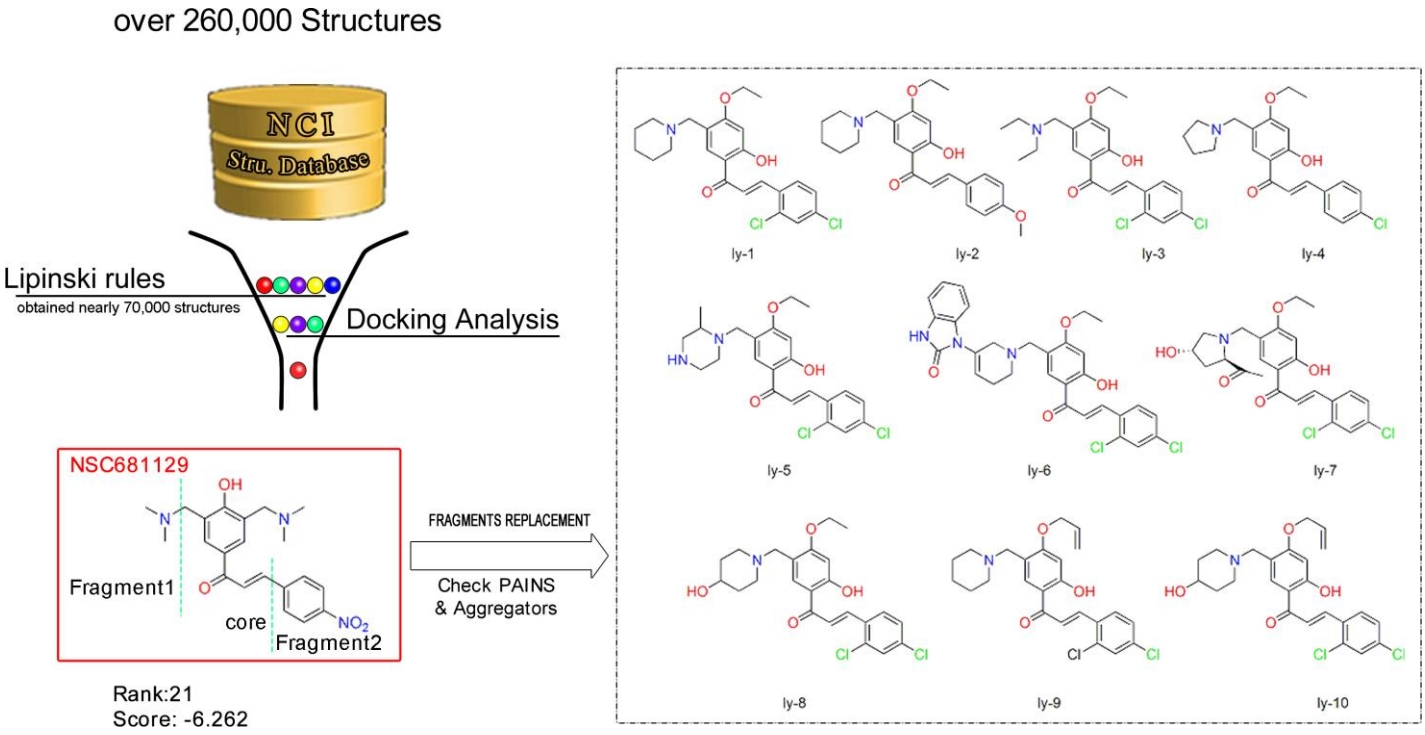

Supplementary Figure S1. CADD *in silico* database screening and structural optimization of a top hit. The drug-like structure database of NCI, USA was screened by using Glide5 of Schrodinger 2010 based on the conformation of the binding pocket (Site 1) of SHP2. NSC681129, ranked 21st in the positive hits identified from the virtual screening, was optimized with other segments from a fragment database. Ten derivatives were generated and passed PAINS and aggregator examination.

Docking results of 10 candidates with SHP2 as the receptor.

		docking score	glide lipo	glide hbond	glide evdw	glide ecoul	glide energy
SHP2							
LY6		-7.34	-3.72	-0.15	-50.18	-7.86	-58.04
LY7		-5.99	-2.10	-0.75	-33.47	-11.35	-44.82
LY8		-5.72	-1.95	-0.59	-37.37	-8.65	-46.03
LY1		-4.93	-2.51	-0.03	-36.78	-3.77	-40.55
LY3		-4.89	-2.43	-0.04	-35.65	-3.94	-39.59
LY9		-4.86	-2.40	-0.05	-35.86	-6.03	-41.88
LY5		-4.68	-2.25	-0.04	-30.99	-5.90	-36.89
LY2		-4.32	-1.71	0.00	-37.67	-3.80	-41.47
LY4		-4.15	-1.21	0.00	-31.70	-7.06	-38.75
LY10		-3.42	-1.33	-0.08	-34.37	-4.91	-39.28

Supplementary Figure S2. Docking results of the 10 derivatives with SHP2 as the receptor. Each molecular candidate was re-docked into the binding site (Site 1) of SHP2 to estimate their binding affinities. The Glide scoring was given based on the sum of water displacement, desolvation effects, and Glide energy including coulomb interaction energy, van der Waals energy, lipophilic and hydrogen-bonding terms, and penalty which included factors that hindered binding.

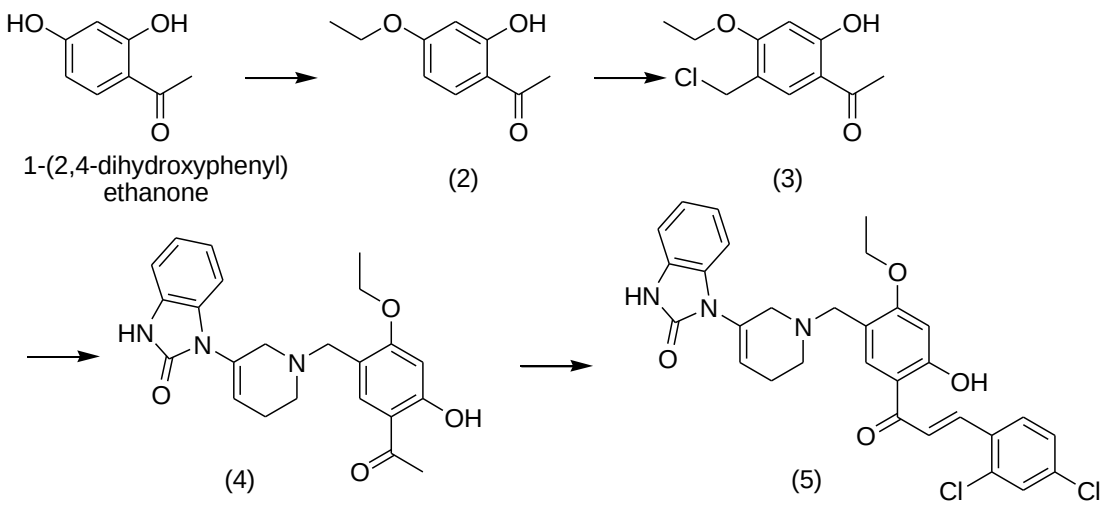

Supplementary Figure S3. Synthetic route of **1**.

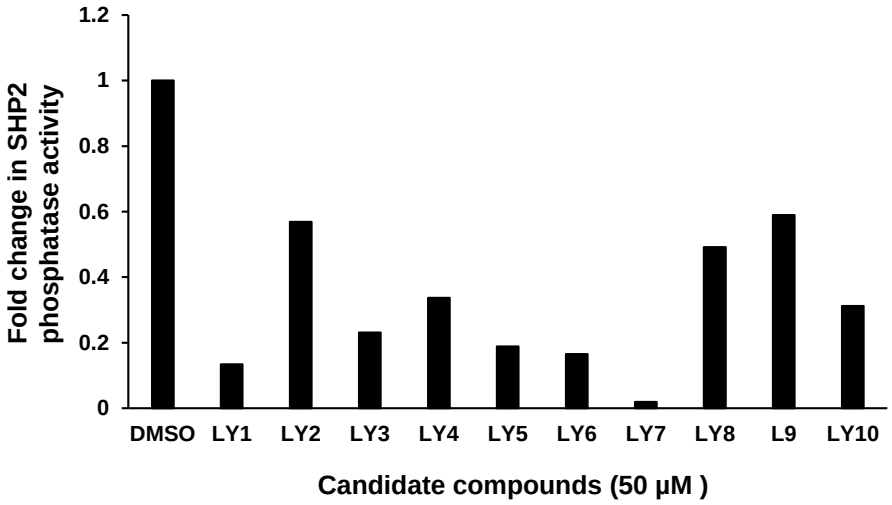

Supplementary Figure S4. Experimental screening data of the ten derivatives. The ten derivative compounds were subjected to the SHP2 phosphatase assay at the concentration of 50 μM, using full length WT SHP2 as the enzyme and a phospho-peptide as the substrate, as described in Experimental Section. DMSO was used as the negative control. Data shown are from one representative experiment.

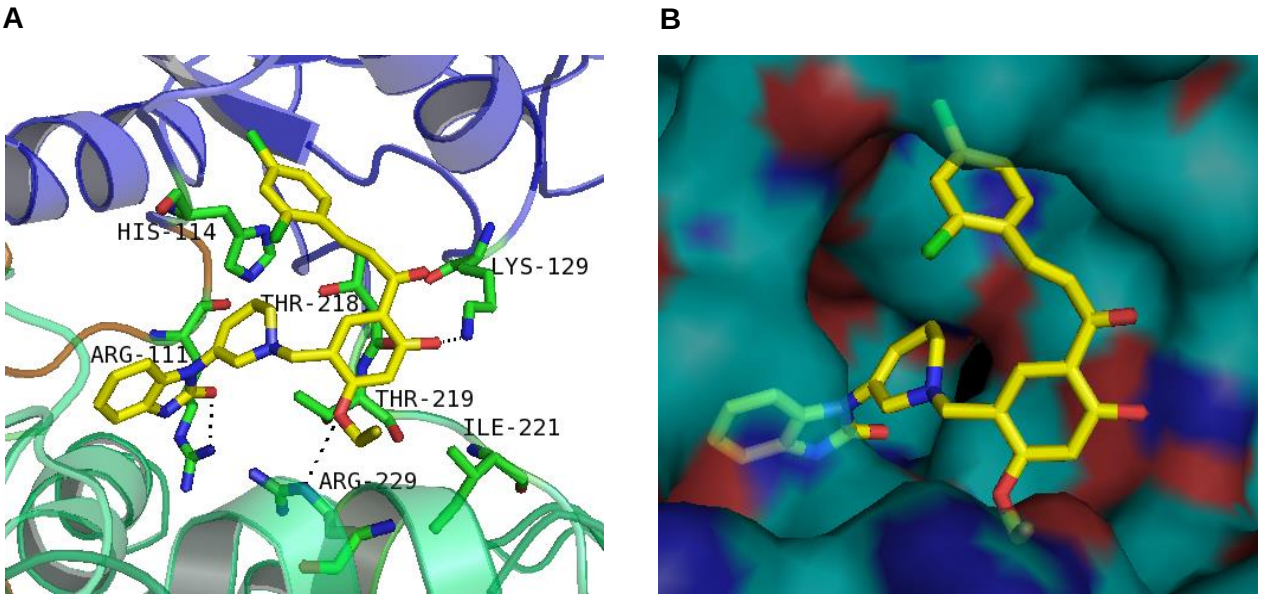

Supplementary Figure S5. Docking pose of **1** and the surface representation of the **1**/SHP2 binding. (A) Docking pose of **1**. **1** is shown in the stick model with the carbon scheme in yellow. **1** forms three hydrogen bonds with Arg111, Lys129, and Arg229. (B) Surface representation of the **1**/SHP2 binding interaction.

A

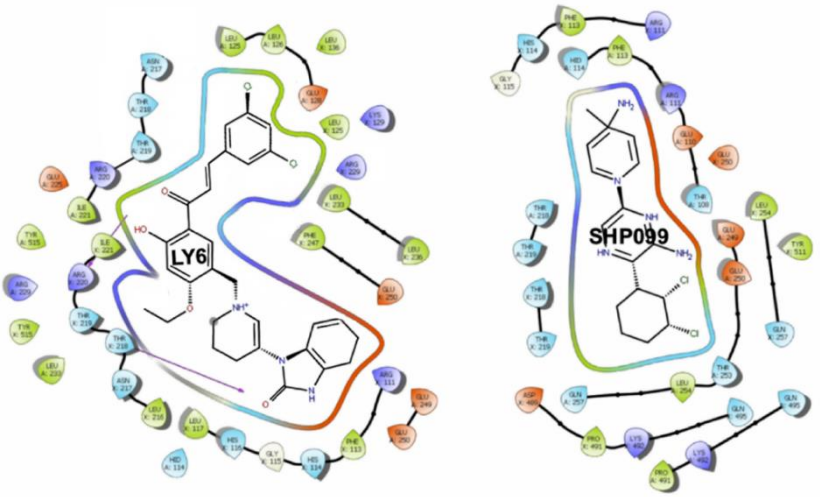

Ligand/protein interaction diagrams of LY6 in Site 1 (left) and SHP099 in SHP-2 (right)

B

Docking score of SHP099 and LY6 with different binding sites

	Docking score	
	Site 1	SHP099 binding site
LY6	-7.3	No poses
SHP099	-4.3	-6.8

Supplementary Figure S6. 1 is predicted to bind to Site 1 in SHP2 with high binding energy. (A) Binding energy was calculated using Glide of Schrodinger with summation of H-bonds interaction (in purple), hydrophobic enclosure (residues in green), charge effects (residues in blue for the negative and red for the positive), etc. for the interaction between **1** and Site 1 of SHP2 with Glide energy of -58.04 kJ/mol, and for the interaction between SHP099 and its binding site (http://www.RCSB.org; PDB ID: 5EHR) with Glide energy of -42.53 kJ/mol. (B) The docking scores for the indicated interactions were calculated with summation of water displacement, desolvation effects, and Glide energy.

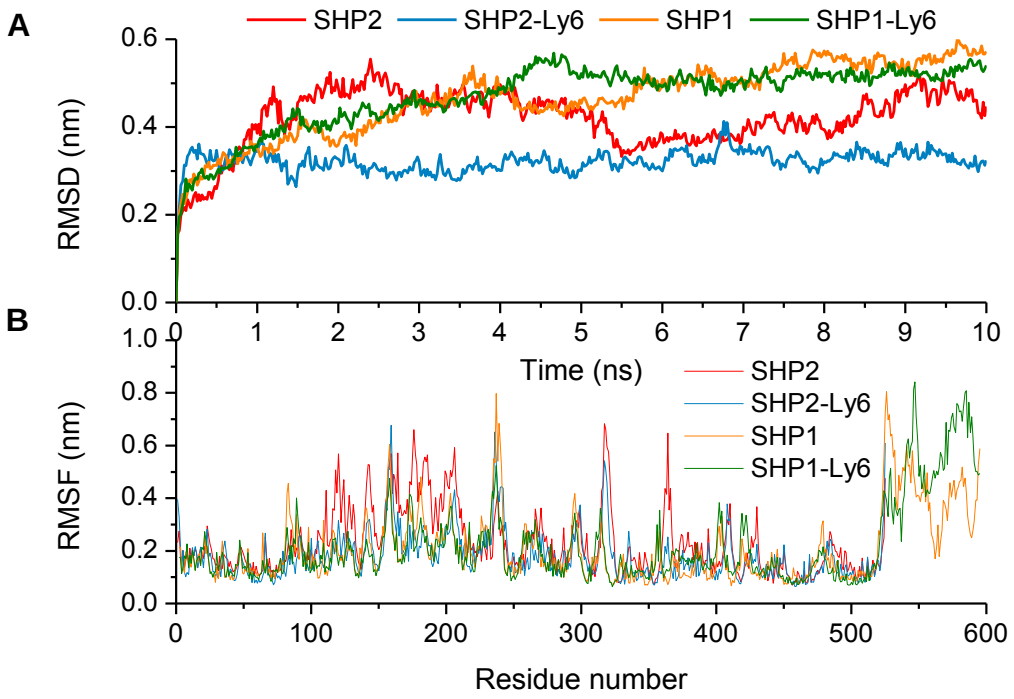

Supplementary Figure S7. Stability analyses of the **1**/SHP2 and **1**/SHP1 complexes. MD simulations were performed for the protein-ligand systems SHP2-**1**, SHP1-**1**, SHP2 alone, and SHP1 alone. (A) RMSD of the four systems over simulation time were determined. (B) RMSF for all the residues of SHP2 and SHP1 were calculated.

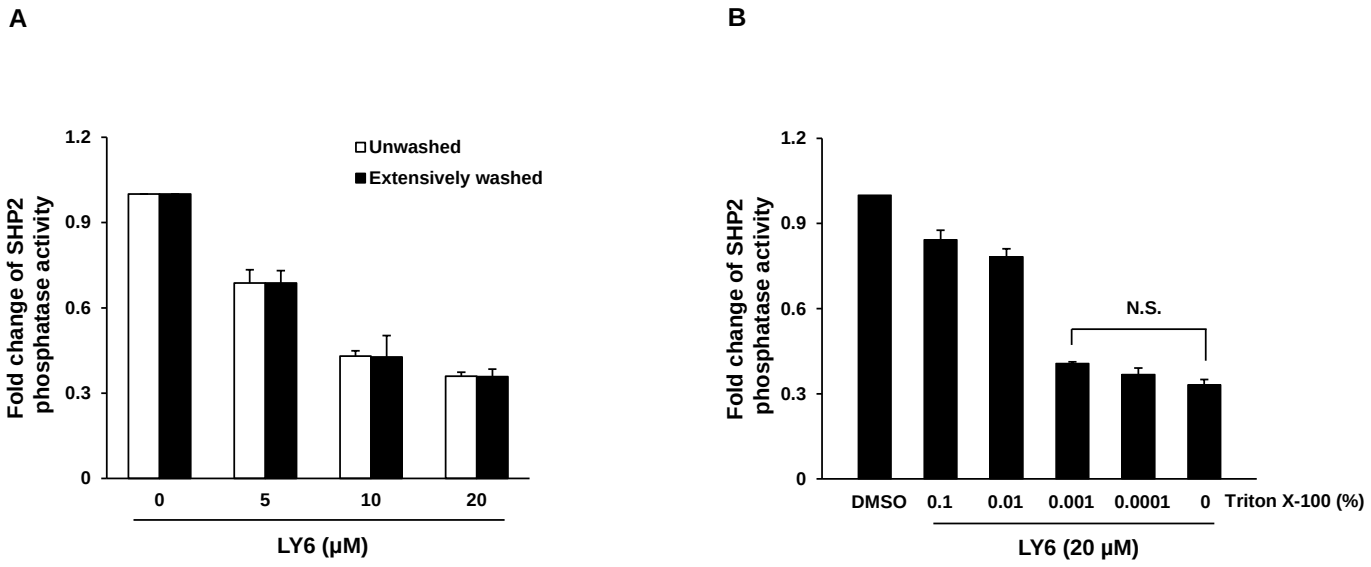

Supplementary Figure S8. 1 is a relatively stable inhibitor of SHP2. (A) GST-full length WT SHP2 (0.1 μg) on glutathione agarose beads was incubated at 4 °C with **1** at the indicated concentrations. Two hours later, beads were collected and washed with the phosphatase assay buffer three times. The phosphatase activity of SHP2 on the beads was determined by the phosphatase assay, as described in Experimental Section. Data are presented as mean ± SD of three independent experiments. (B) **1** (20 μM) was tested by the phosphatase assay, as described above, in the presence of Triton X-100 at the indicated concentrations. Results shown are mean ± SD of three independent experiments.

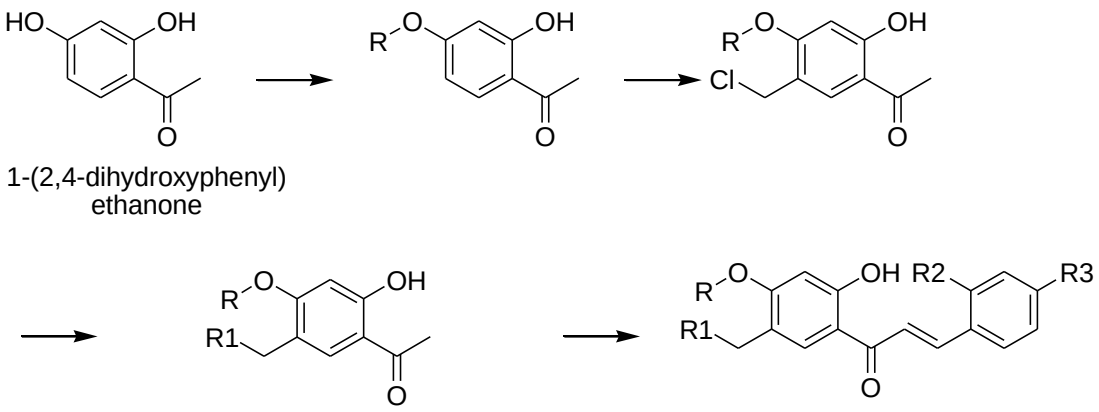

	R	R1	R2	R3
LY1	ethyl	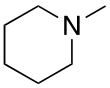	Cl	Cl
LY2	ethyl	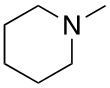	H	OCH_3
LY3	ethyl	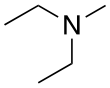	Cl	Cl
LY4	ethyl	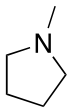	H	Cl
LY5	ethyl	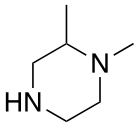	Cl	Cl

	R	R1	R2	R3
LY7	ethyl	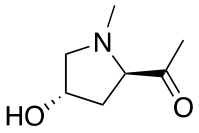	Cl	Cl
LY8	ethyl	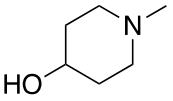	Cl	Cl
LY9	allyl	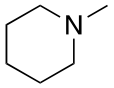	Cl	Cl
LY10	allyl	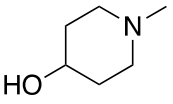	Cl	Cl

Supplementary Figure S9. Synthesis of other derivative compounds than **1**.

Derivatives LY1-LY5, LY7, and LY8 were synthesized using 1-(2,4-dihydroxyphenyl) ethan-1-one and

diethyl sulfate as starting materials with 4-step reactions. Synthetic steps 1-3 of these compounds were exactly same as those of **1** described in Experimental Section. For the synthesis of LY9 and LY10, different starting materials [1-(2,4-dihydroxyphenyl) ethan-1-one and 1,4-dibromo butane] were used at Step 1, but the same synthetic route was followed (see details below).

Building blocks (2 and 3) for LY9 and LY10. Anhydrous potassium carbonate (0.138g, 1 mmol) was added to the solution of 1-(2,4-dihydroxyphenyl) ethan-1-one (0.152g, 1 mmol) in DMSO (10 mL), and the solution was stirred continuously in the inert atmosphere (helium gas). 1,4-dibromo butane (0.12g, 1 mmol) was slowly dropped into the above yellow solution. The reaction mixture was stirred for extra 2 hours. The completion of the reaction was monitored by TLC. The reaction mixture was extracted with ethyl acetate (5 mL) and washed three times with ice cold water. The organic layer was treated with anhydrous sodium sulfate. The products [Building blocks (2)] were directly used for the next step without further purification. They were added into the solution of chloromethyl methyl ether (1.40g, 12.2 mmol) and diluted in 10 mL acetic acid and stirred at ambient temperature for 24 hours. Building blocks (3) for LY9 and LY10 (77.3mg, 0.3 mmol) were obtained with yield of 29.5%.

Building blocks (4). Piperidine for LY1, LY2, and LY9 (4.3g, 51.0mmol), diethylamine for LY3 (3.7g, 51mmol), pyrrolidine for LY4 (3.6g, 51 mmol), 2-methylpiperazine for LY5 (5.1g, 51 mmol), 1-((2R,4S)-4-hydroxypyrrolidin-2-yl) ethan-1-one for LY7 (6.6g, 51 mmol), and piperidin-4-ol for LY8 and LY10 (5.2g, 51 mmol) were added into the solution of Building block (3) (7.7g, 33.6 mmol) in 30 mL ethyl acetoacetate at room temperature and stirred for 24 hours with K_2CO_3 (1.74g, 12.6 mmol). The solvent was removed under reduced pressure, and then washed with brine and 1 M hydrochloric

acid 3 times, respectively. The solution was extracted with ethyl acetoacetate after adjusting pH to 8-9 with 1 M K_2CO_3. After the volatile solvent of the reaction was evaporated, yellow pale oily raw products [Building blocks (4)] were obtained.

Final products. Building Blocks (4) (LY1: 645.2mg, 2.5mmol; LY2: 700.5mg, 2.5 mmol; LY3: 615.3mg, 2.5 mmol; LY4: 612.8mg, 2.5 mmol; LY5: 686.0mg, 2.5 mmol; LY7: 680.3mg, 2.5 mmol; LY8: 685.3mg, 2.5 mmol; LY9: 675.3mg, 2.5 mmol; LY10: 717.8mg, 2.5 mmol) were mixed with 2,4-dichlorobenzaldehyde (0.88g, 5 mmol) for LY1, LY3, LY5, and LY7-LY10, p- dichlorobenzaldehyde (0.7g, 5 mmol) for LY4, and 4-methoxypiperidine (0.6g, 5 mmol) for LY2, and KOH (0.7g, 12mmol). The mixtures were stirred in 9 mL ethanol and 2 mL water at room temperature for 24 hours. Final products were isolated by solvent-extraction followed by column chromatography. The purity and chemical structures of these final compounds were determined by HPLC and NMR, respectively (Supplementary HPLC and NMR results).